JOURNAL OF CATALYSIS **173,** 105–114 (1998)
ARTICLE NO. CA971912

Isomerization of 1-Butene over Silica-Supported Mo(VI), W(VI), and Cr(VI)

Narayanan C. Ramani, David L. Sullivan, and John G. Ekerdt

Department of Chemical Engineering, University of Texas, Austin, Texas 78712

Received January 21, 1997; revised September 23, 1997; accepted September 24, 1997

Isomerization of 1-butene on Mo(VI)/SiO_2, W(VI)/SiO_2, and Cr(VI)/SiO_2 was investigated by steady-state flow reactor studies and Fourier transform infrared spectroscopy. (η^5-$C_5H_5)_2M_2(CO)_6$ or M(η^3-$C_3H_5)_4$ (M = Mo, W) were used as precursors in preparing Mo(VI)/SiO_2 and W(VI)/SiO_2 catalysts. $Cr(NO_3)_3$ was used to prepare Cr(VI)/SiO_2. Isomerization proceeds by a Brønsted catalyzed pathway involving alkoxide intermediates and an oxidative dehydrogenation pathway involving allylic intermediates. Flow reactor experiments revealed that two pathways for isomerization could be observed with Mo(VI)/SiO_2: through the alkoxide intermediate at $T < 523$ K and through the allylic intermediate at $T > 573$ K. W(VI)/SiO_2 catalysts were more active for isomerization than Mo(VI)/SiO_2 catalysts, but the demarcation of the two pathways was not as clear. Only the oxidative dehydrogenation pathway for isomerization was observed for the Cr(VI)/SiO_2 catalysts at $T > 473$ K. In IR studies, alkoxide intermediates were observed following adsorption of 1-butene on Mo(VI)/SiO_2 and W(VI)/SiO_2 catalysts at 300 K; complete desorption of the surface alkoxide occurred by 523 K. The surface species observed for adsorption of 1-butene on Cr(VI)/SiO_2 at 300 K were typical of allylic C–H abstraction; these surface species transform into deep oxidation products on heating, resulting in a surface that is poisoned. Pyridine adsorption studies reveal traces of Brønsted acidity on Mo(VI)/SiO_2, W(VI)/SiO_2, and Cr(VI)/SiO_2. Brønsted acidity would account for the alkoxide mechanism of 1-butene isomerization. The reason that these Brønsted acid sites are most active for 1-butene isomerization on W(VI)/SiO_2 and inactive on Cr(VI)/SiO_2 is discussed.

INTRODUCTION

Butadiene is used primarily in the polymer industry for making styrene–butadiene rubber, and is synthesized by the oxidative dehydrogenation of 1-butene (1, 2). This reaction proceeds through an allylic intermediate, with two C–H abstractions required for product formation. Mixed metal oxides such as bismuth molybdates and iron oxides are typically used as industrial catalysts (3, 4). Many factors such as cation reducibility, oxygen ligand type (oxo M=O or bridging M–O–M′), structure (isolated cations, oligomers, or crystallites), and acidity of the catalyst could affect the activity and selectivity of the reactions involving C–H bond scission. Isomerization of butenes and oxidation to 1,3-butadiene could take place through a common allylic intermediate. The presence of a common intermediate would mean that selectivity to butene isomers or 1,3-butadiene would reflect the relative ease of the different C–H abstraction steps. The focus of this paper is on understanding the pathways for isomerization of butenes over well-characterized model oxide catalysts, where the roles of cation structure, reducibility, and acidity can be explored. The oxidative dehydrogenation of 1-butene to 1,3-butadiene will be discussed in greater detail in a subsequent publication (5).

Adsorption and reaction of alkenes have been widely studied on a variety of oxide surfaces (6–8). The primary focus, though, has been on ethylene and propylene, which are simpler probe molecules. Metathesis of 1-butene on reduced oxide surfaces is also well understood (9, 10), but relatively few studies have addressed adsorption and reaction on fully oxidized surfaces. Figure 1 shows the possible ways that 1-butene interacts with oxide surfaces. If 1-butene adsorbs molecularly, it forms a π complex on the surface, with the C=C bond coordinated to the supported cation (Lewis acid site). If Brønsted acid sites are present, then protonation of 1-butene can occur, resulting in an alkoxide intermediate (carbenium ion) where the C=C character has been lost. Subsequent loss of a proton from a different carbon atom results in isomerization. If the first step involves C–H bond cleavage, an allylic intermediate is formed, with a resonant C–C–C bond coordinated to a supported metal atom. Subsequent hydrogenation at a different carbon atom results in isomerization. On the other hand, a second C–H bond cleavage results in 1,3-butadiene, the selective oxidation product. Thus, there are two main mechanisms by which isomerization of 1-butene could take place, through the alkoxide or through the allylic intermediate.

Kokes and co-workers reported both π complexes of butenes and allylic intermediates in the adsorption of 1-butene on ZnO (7, 11). π complexes of butenes have also been observed on silica, Na–Y zeolites, and TiO_2 during low-temperature studies (12). More recently, Busca and co-workers have studied 1-butene adsorption and

0021-9517/98 $25.00

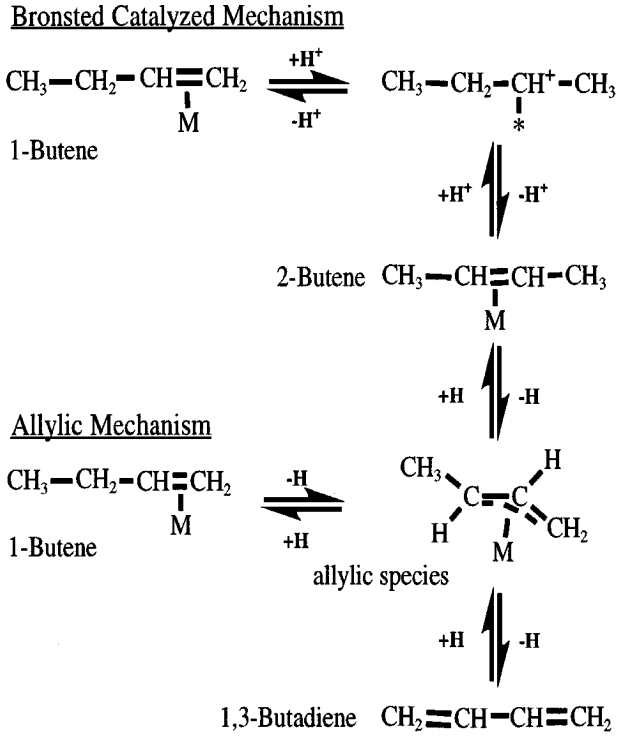

FIG. 1. Reaction scheme for isomerization and dehydrogenation of 1-butene.

reaction on $FeCrO_3$, $MgFe_2O_4$, V_2O_5/TiO_2, and vanadyl pyrophosphates (6, 13–15). On V_2O_5/TiO_2, room temperature adsorption and temperature evolution led to the formation of *sec*.-butoxide species that transformed to ethyl methyl ketone and, subsequently, to acetate species. On $FeCrO_3$, two pathways were reported; the first involving *sec*.-butoxides that transformed to ethyl methyl ketone, and the second involving an allylic intermediate that led to the formation of methyl vinyl ketone and 1,3-butadiene. The allylic intermediate could not be observed and it was suggested that it reacted rapidly to form methyl vinyl ketone and 1,3-butadiene. Pathways to isomerization were not studied.

Our goal is to understand the role of acidity, structure, and cation reducibility in C–H reactions, and our approach is to study these reactions over well-characterized Cr(VI), Mo(VI), and W(VI) oxides supported on SiO_2. Silica is a relatively inert support, so the supported cation chemistry can be easily examined. All three supported cations are group VIB transition metals, with cation reducibility decreasing down the group (Cr > Mo > W). Organometallic preparation routes enable higher dispersion of Mo and W than previously possible on SiO_2 (7, 11, 16–18). The surface structures of these supported metal oxides have been extensively investigated by a variety of spectroscopic techniques including Raman spectroscopy, X-ray photoelectron spectroscopy, extended X-ray absorption fine-structure spectroscopy, and ultraviolet diffuse reflectance spectroscopy, and a detailed picture has emerged (19–26). Under fully oxidized and dehydrated conditions, Mo and W cations are present in a distorted octahedral geometry, with one oxo oxygen ligand (M=O) and four bridging oxygen ligands (M–O–M′). Recent studies support a similar structure for the dispersed Cr cation (27).

While surface structures of supported metal oxides have been extensively characterized, there is still some disagreement in the literature about the presence of Brønsted acidity on silica-supported metal oxides (28–30). Understanding Brønsted acidity is important since isomerization of 1-butene could occur by a Brønsted catalyzed pathway. Pyridine adsorption has been widely used as a probe molecule to investigate Brønsted and Lewis acidity (4, 9, 31–33). Dumesic and co-workers have reported Brønsted acidity on 6.4% Mo/SiO_2, but not for 1% Mo/SiO_2 (29). MoO_3 crystallites were present at the higher weight loading and it was suggested that the hydroxyl groups associated with the crystallites were the Brønsted acid sites. Rajagopal *et al*., on the other hand, report no Brønsted acidity up to 12% MoO_3/SiO_2, even when MoO_3 crystallites were present (28). It is possible that their samples were partially reduced since their pretreatment was done with He flow at 773 K. Datka and co-workers observed Brønsted acidity on Nb_2O_5/SiO_2 when the weight loading was more than 4% (34). Crystallites of Nb_2O_5 were present at these weight loadings. They suggested a hydroxyl group that was bridging a Nb cation and a Si atom was responsible for Brønsted acidity. As yet, no studies have been carried out over fully dispersed, fully oxidized Mo, W, or Cr oxides supported on SiO_2.

METHODS

Silica-supported Mo(VI) and W(VI) oxides were prepared by an organometallic route using either $(\eta^5\text{-}C_5H_5)_2M_2(CO)_6$ or $M(\eta^3\text{-}C_3H_5)_4$ (M = Mo, W). Details of the preparation method have been reported previously (16, 18). The precursors attach to the SiO_2 surface by reaction with the hydroxyl groups, and after removal of the organic ligands, the supported metal oxide formed is in a reduced oxidation state. The samples are then fully oxidized at 773 K in a flow of hydrocarbon free air (HFA) for 8 h. The supported $Cr(VI)/SiO_2$ samples were prepared through an incipient wetness technique using $Cr(NO_3)_3$, followed by calcination at 773 K in HFA for 8 h. The SiO_2 used in these preparations was Cab-O-Sil HS 5 (325 m^2/g). The objective of using these preparation methods was to obtain supported metal oxides where isolated cations in the 6+ oxidation state could be obtained, without crystallites, as had been previously reported (16, 25). X-ray diffraction studies indicated that crystallites of WO_3, MoO_3, or Cr_2O_3 were not present on the respective samples. Raman spectroscopy was carried out at Lehigh University on a Spex Triplemate (Model 1877)

spectrometer using an Ar^+ ion laser (Spectra Physics 2020-50) delivering about 15–50 mW of incident radiation. While surface species consisting of isolated cations in the 6+ oxidation state were observed for all three supported metal oxides, crystallites of WO_3 were also observed for the $W(VI)/SiO_2$ sample (5). Raman spectroscopy is generally more sensitive than X-ray diffraction for probing crystallites of supported metal oxides. The surface area of the catalysts was characterized by BET and did not vary appreciably from that for the SiO_2. The weight loadings of the catalysts were 4.1 and 6.5% for $Mo(VI)/SiO_2$, 5.4% for $W(VI)/SiO_2$, and 1% for $Cr(VI)/SiO_2$. Weight loadings for Mo and Cr were obtained by atomic absorption spectroscopy and the weight loading for W was determined by Galbraith Laboratories. The 6.5% $Mo(VI)/SiO_2$ catalyst was used for the Fourier transform infrared (FTIR) studies as it provided more sites on which 1-butene adsorption could take place and, consequently, a better signal.

The flow reactor experiments were performed in a 0.5-mm-i.d. quartz U-tube reactor. Approximately 50 to 100 mg of sample was used for each run. The samples were first calcined in HFA at 773 K for 3 h before being cooled to 473 K in HFA. Then a flow of 20 sccm (standard cm^3/min) of 5000 ppm 1-butene in He and 5 sccm of 2% O_2 in He was started. The flow rates were such that a 1 : 1 molar ratio of 1-butene to O_2 was present (7.4×10^{-8} mol 1-butene/s and 7.4×10^{-8} mol O_2/s). The system was allowed to stabilize for 1 h. The temperature was lowered again to 300 K and allowed to stabilize for at least 30 min before data were collected. The temperature was sequentially increased to the next value. The rate measurements were made under differential conditions and conversions were below 20% for all samples. At the end of each run, the activity was measured again at the initial temperature to ensure that the catalyst surface had not changed with thermal treatment. For selected samples, data were collected while both sequentially increasing and decreasing the temperature, to ensure that there were no hysteresis effects. The data agreed to within 5%. The reaction was also tested for equilibrium limitations and was found to be independent of gas flow rates. During these measurements, the concentrations of 1-butene and O_2 were the same, as the flow rates of the respective feed gases were increased proportionately. The effluent from the reactor was sampled on-line with a Hewlett–Packard 5880A gas chromatograph (GC) equipped with a flame ionization detector and a thermal conductivity detector. An SP 1700 column was used to separate the hydrocarbons, and a combination of a 5-Å molecular sieve column and a PoraPLOT Q column was used to separate CO and CO_2. Certified gas mixtures from Matheson and Liquid Carbonic Industries were used to calibrate detector sensitivities and retention times for reactants and products.

The IR experiments were performed with a Mattson Research Series 1 spectrometer equipped with a mercury–cadmium–telluride detector. Spectra were obtained with a resolution of 1 cm^{-1} and 100 scans. The IR cell used in these experiments has been described previously (35). It consisted of two heated zones, one for high-temperature calcination up to 873 K and another in which *in situ* heating up to 623 K could be performed. A desired gas mixture could be passed through the cell via a gas manifold, or the cell could be evacuated to a pressure of 50 mTorr. All gases used were certified gas mixtures from Matheson. Oxygen and moisture traps were used appropriately. A self-supporting wafer of the sample was dehydrated at 773 K in HFA and cooled to room temperature in HFA. The cell was evacuated, and a 5000-ppm 1-butene in He mixture was introduced at a flow rate of 20 sccm. After 5 min, the cell was evacuated and the spectra were taken. Temperature evolution studies were carried out from 300 to 623 K. Pyridine adsorption studies were carried out in the same cell. Pyridine was delivered to the cell with a doser that contained predried molecular sieves to remove any water. After pyridine dosing, the cell was evacuated and heated to 473 K to remove pyridine that was hydrogen bonded to the SiO_2, and spectra were taken.

RESULTS

Figure 2 shows typical activity data for formation of 2-butenes and 1,3-butadiene as a function of temperature for

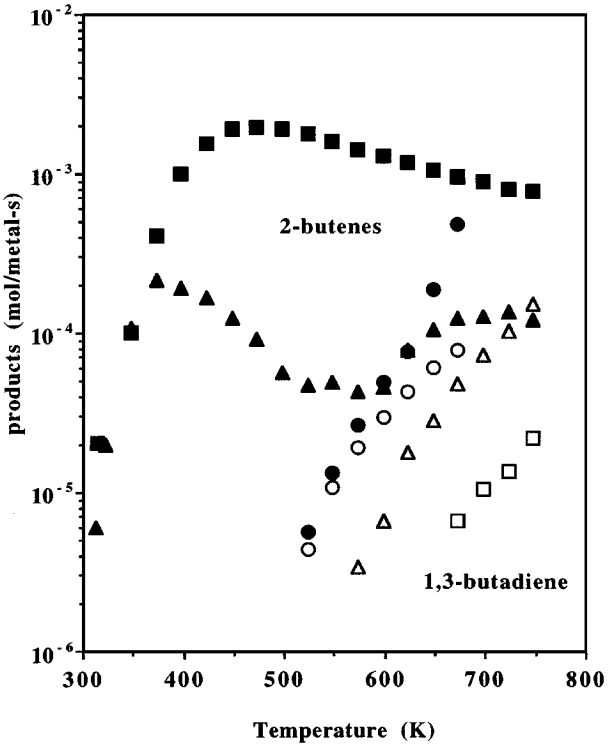

FIG. 2. Rate of isomerization and oxidation of 1-butene over silica-supported Mo(VI) (▲, △); W(VI) (■, □); and Cr(VI) (●, ○) oxides.

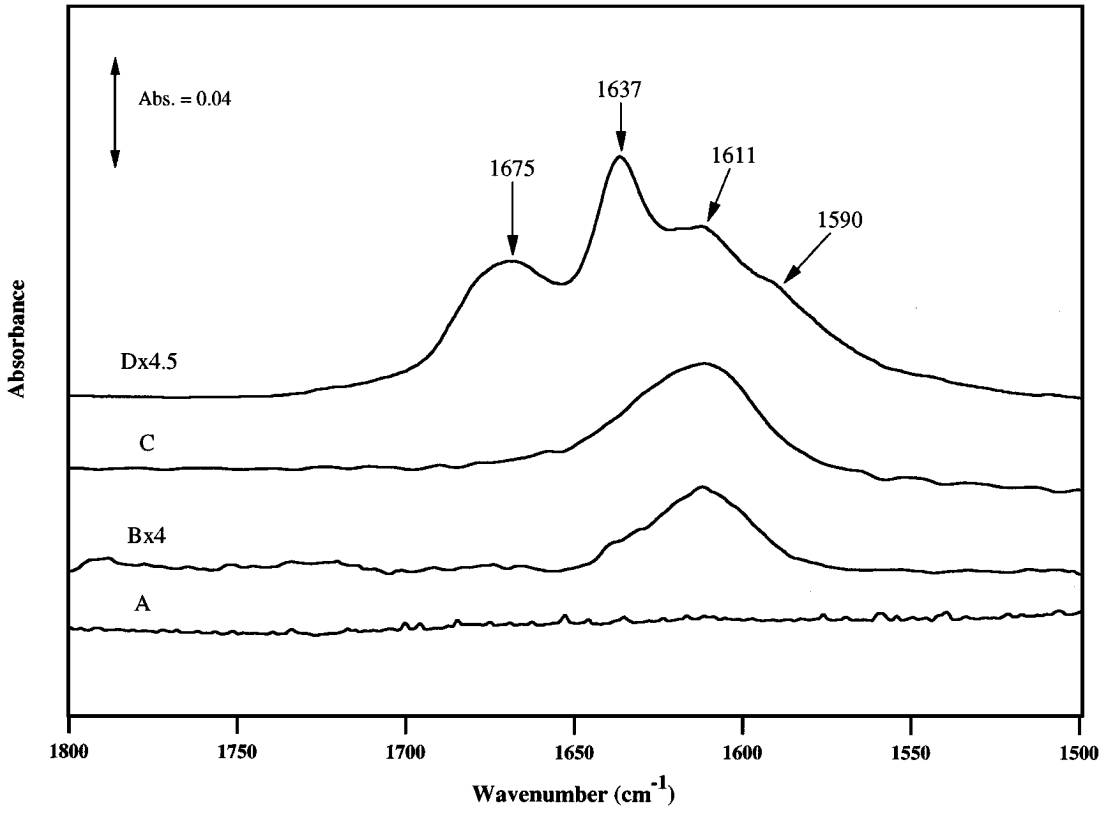

FIG. 3. Adsorption of 2-butanol on Mo(VI)/SiO_2 at 300 K (A) and adsorption of 1-butene at 300 K on Mo(VI)/SiO_2 (B), W(VI)/SiO_2 (C), and Cr(VI)/SiO_2 (D).

silica-supported Mo(VI), W(VI), and Cr(VI) catalysts. A small amount of 2-butenes (1.1×10^{-9} mol/s) was present as an impurity in the 1-butene feed, and this was subtracted out in the data analysis. Activity is normalized by total metal present. Mo and Cr are fully dispersed as isolated cations (5). Small WO_3 crystallites are present along with isolated W cations; therefore, the turnover numbers for W(VI) may be underestimated in Fig. 2. For Mo(VI)/SiO_2 and W(VI)/SiO_2, isomerization activity is observed well before oxidation. For Mo(VI)/SiO_2, two distinct mechanistic regimes for isomerization can be seen. Isomerization activity reaches a peak at 400 to 425 K and increases again with the onset of oxidation at 573 K. On W(VI)/SiO_2 this demarcation is not as clear, as isomerization activity reaches a maximum around 473 K but does not drop significantly at higher temperatures. Over Cr(VI)/SiO_2, isomerization activity is observed only with the onset of 1,3-butadiene formation at 523 K. The *cis/trans* ratios for the Cr(VI)/SiO_2, Mo(VI)/SiO_2, and W(VI)/SiO_2 samples were between 1.1 and 1.7 over the entire temperature range studied. There was no apparent temperature dependence of the *cis/trans* ratios. The onset of oxidation activity (1,3-butadiene formation) is at 523 K for Cr, 573 K for Mo, and 673 K for W supported on SiO_2 under these reaction conditions. Activation energies for 2-butene formation could not be accurately estimated since two different mechanistic regimes are present in the temperature range studied. For 1-butene oxidation to 1,3-butadiene, activation energies were between 30 and 35 KJ/mol.

Figures 3 and 4 show IR spectra of 1-butene adsorbed on Mo(VI)/SiO_2, W(VI)/SiO_2, and Cr(VI)/SiO_2 at 300 K in the C=C stretching and C–H stretching regions, respectively. In the C=C stretching region, 1-butene adsorption on Cr(VI)/SiO_2 results in three distinct bands at 1611, 1637, and 1675 cm^{-1}. A weak shoulder at 1590 cm^{-1} is also observed. On W(VI)/SiO_2, only one strong band is observed at 1611 cm^{-1}. On Mo(VI)/SiO_2, a comparatively weaker band is observed at 1611 cm^{-1}. Other smaller features observed above 1700 cm^{-1} and below 1550 cm^{-1} result from smoothing of data and noise, and are not from adsorbed species. The noise in these regions arises from very small differences in the amount of water in the beam path for the sample and the background that cannot be properly subtracted. In the C–H stretching region (Fig. 4), strong bands at 2980, 2940, 2931, and 2885 cm^{-1} are observed on Mo(VI)/SiO_2 and W(VI)/SiO_2 and are characteristic of sp^3-hybridized CH_3 and CH_2 stretching modes (36). A weak band observed at 2860 cm^{-1} is consistent with the overtone of the CH_3 bending mode. On Cr(VI)/SiO_2, very weak bands are observed at the same frequencies. Vinylic C–H

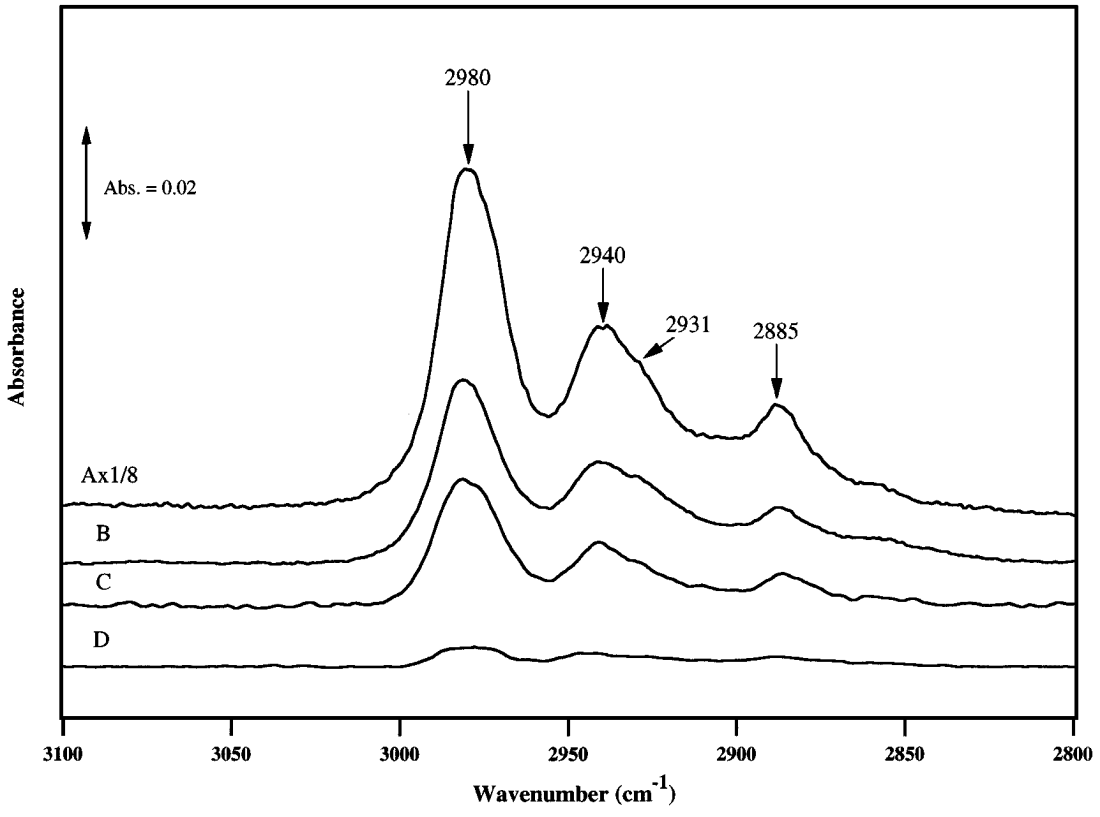

FIG. 4. Adsorption of 2-butanol on Mo(VI)/SiO_2 at 300 K (A) and adsorption of 1-butene at 300 K on Mo(VI)/SiO_2 (B), W(VI)/SiO_2 (C), and Cr(VI)/SiO_2 (D).

stretching modes between 3000 and 3100 cm^{-1} are not observed for any of the samples. The spectrum of 2-butanol adsorbed on Mo(VI)/SiO_2, which is expected to form 2-butoxide, is presented in Figs. 3 and 4 for comparison.

Figure 5 shows IR spectra of surface species in the C–H stretching region for Mo(VI)/SiO_2 as a function of temperature. By 473 K, the adsorbed surface species that is observed at 300 K has essentially desorbed. In the C=C stretching region (not shown), the weak band at 1611 cm^{-1} followed a similar trend and disappeared by 473 K. Temperature evolution of adsorbed 1-butene on W(VI)/SiO_2 (not shown) is analogous to that in the Mo(VI)/SiO_2 system. On Cr(VI)/SiO_2, the temperature evolution is shown in Fig. 6 for the C=C stretching region since the strongest IR bands are present in this region, and if allylic intermediates form, absorbances are expected in this region. The 1675, 1637, and 1611 cm^{-1} bands observed at 300 K have been assigned to C=C stretching modes of adsorbed butenes. With increasing temperature, the bands at 1675 and 1611 cm^{-1} increased in intensity, and new bands emerged simultaneously at 1590 and 1560 cm^{-1}. By 573 K, the bands above 1600 cm^{-1} diminished while the broad peak centered at 1560 cm^{-1} further increased in intensity along with the emergence of another broad feature centered at 1425 cm^{-1}. These two bands are very intense and broad and are characteristic of oxygenated hydrocarbons. Our results show that adsorbed 1-butene undergoes transformations on the Cr(VI)/SiO_2 surface instead of desorbing.

Pyridine adsorption experiments were carried out to determine whether any Brønsted acidity was detectable on the silica-supported metal oxides at $T < 500$ K; the results are presented in Fig. 7 and the band assignments are listed in Table 1. On SiO_2, the 8a and 19b modes of adsorbed pyridine were observed at 1595 and 1445 cm^{-1},

TABLE 1

Assignment of the Main Infrared Bands of Adsorbed Pyridine[a]

	Pyridine on Lewis acid sites (cm^{-1})				Pyridinium ion on Brønsted acid sites (cm^{-1})	
	8a[b]	8b	19a	19b	8a	19b
Cr(VI)/SiO_2	1609	1575	1489	1449	1637	1542
Mo(VI)/SiO_2	1611	1577	1490	1452	1638	1538
W(VI)/SiO_2	1613	1577	1490	1453	1639	1543

[a] Hydrogen-bonded pyridine on SiO_2 has the 19b and 8a ring vibrational modes at 1445 and 1595 cm^{-1}, respectively.

[b] 8a, 8b, 19a, and 19b are ring vibrational modes of pyridine proposed by Kline and Turkevich (37).

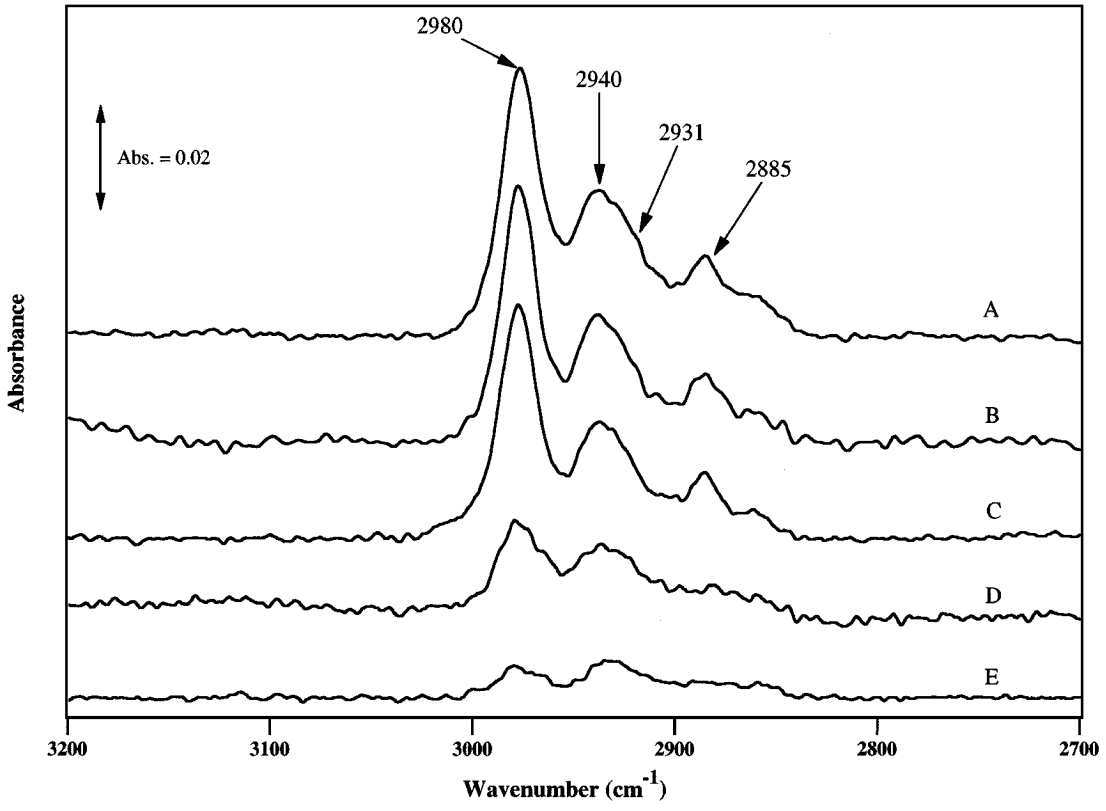

FIG. 5. Temperature evolution of 1-butene adsorbed on Mo(VI)/SiO_2 at (A) 300 K, (B) 323 K, (C) 373 K, (D) 423 K, and (E) 473 K.

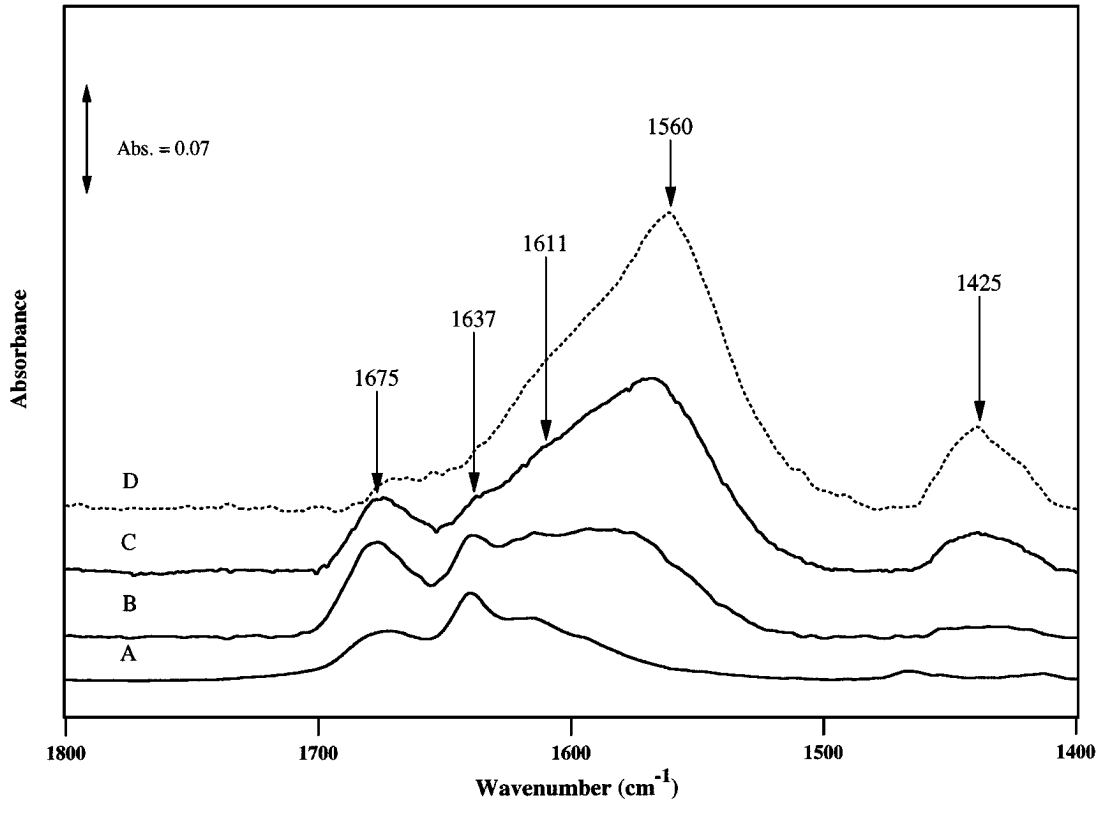

FIG. 6. Temperature evolution of 1-butene adsorbed on Cr(VI)/SiO_2 at (A) 300 K, (B) 423 K, (C) 473 K, and (D) 573 K.

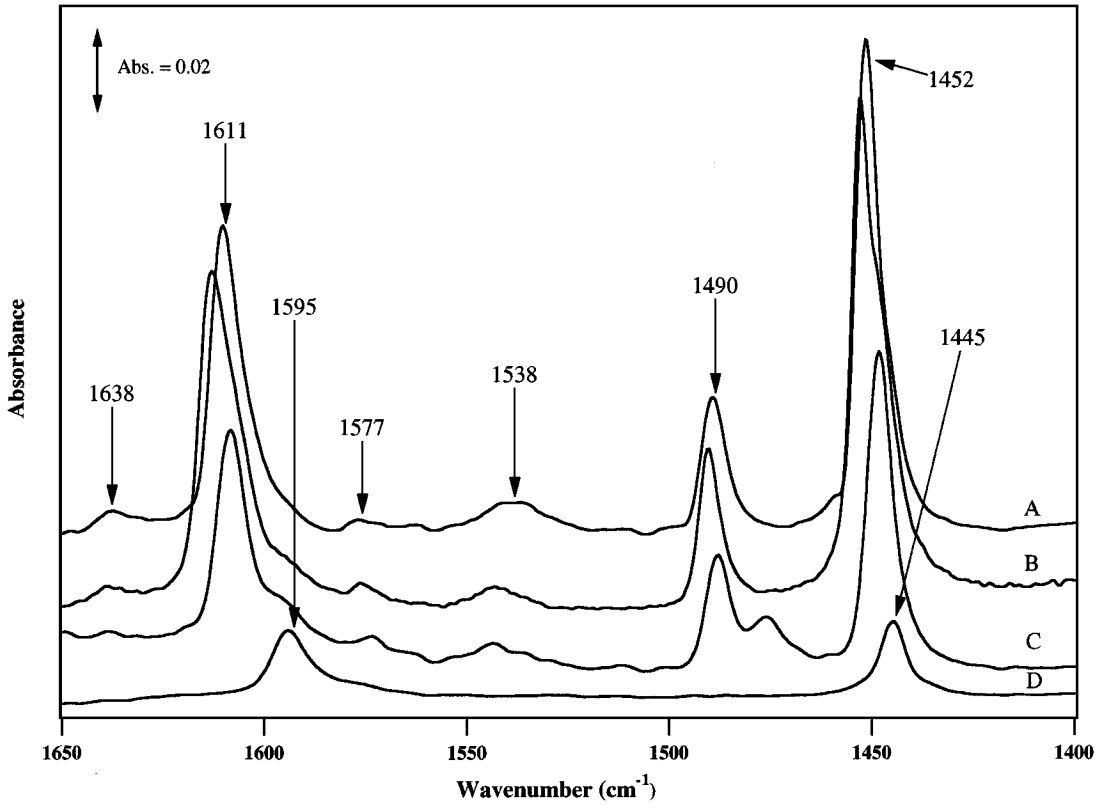

FIG. 7. Adsorption of pyridine at 473 K on (A) W(VI)/SiO_2, (B) Mo(VI)/SiO_2, (C) Cr(VI)/SiO_2, and (D) Cab-O-Sil SiO_2 immediately after evacuation at 473 K.

respectively, and are characteristic of hydrogen-bonded species. After 15 min of evacuation, all the pyridine desorbs, leaving behing a clean SiO_2 surface. On Mo(VI)/SiO_2, predominantly Lewis acidity characterized by bands at 1611, 1490, and 1452 cm^{-1} and some Brønsted acidity with pyridinium ion ring vibration modes at 1638 and 1538 cm^{-1} are observed. The results on W(VI)/SiO_2 are similar to those on Mo(VI)/SiO_2 but the Brønsted acidity is much more evident, with broad bands at 1639 and 1543 cm^{-1}. On Cr(VI)/SiO_2, bands corresponding to pyridine coordinated to Lewis acid sites are observed at 1609, 1575, 1489, and 1449 cm^{-1} while the pyridinium ion bands at 1637 and 1542 cm^{-1} are extremely weak. Another band at 1470 cm^{-1} is observed on the Cr(VI)/SiO_2 sample that is possibly from a 2,2-bipyridyl group produced by pyridine oxidation (38).

DISCUSSION

Isomerization of 1-butene can take place through a Brønsted catalyzed pathway involving alkoxide intermediates or through an allylic pathway where C–H abstraction is the first step (Fig. 1). The presence of Brønsted acidity on the catalyst surface is essential for isomerization through an alkoxide intermediate. Our pyridine adsorption experiments (Fig. 7) on Mo(VI)/SiO_2, W(VI)/SiO_2, and Cr(VI)/SiO_2 indicate that small amounts of Brønsted acid sites are indeed present on these catalysts. Therefore, a Brønsted catalyzed pathway for the isomerization of 1-butene must be considered when interpreting the reaction data. In previous work on silica-supported Mo, V, and Nb oxides, Brønsted acidity was reported at higher metal weight loadings, where crystallites of MoO_3, V_2O_5, and Nb_2O_5 are present (29, 34). In our studies, the Mo(VI)/SiO_2 and Cr(VI)/SiO_2 catalysts contained well-dispersed cations in the isolated and fully oxidized (6+) state (5). On W(VI)/SiO_2, both crystallites of WO_3 and isolated cations of W are present. While the contribution of WO_3 crystallites to the Brønsted acidity on W(VI)/SiO_2 is possible, the presence of Brønsted acidity on Mo(VI)/SiO_2 and Cr(VI)/SiO_2 indicates that such acidity can be associated even with well-dispersed cations. For isomerization of 1-butene via the allylic pathway, C–H abstraction is the first step. Cations that can be easily reduced and reoxidized are known to be highly active in such allylic C–H abstraction reactions (2, 4). In our experiments, the three cations studied (W, Mo, and Cr) have increasing reducibility. It can therefore be expected that the allylic pathway over the Cr(VI)/SiO_2 catalysts should be easier than those over Mo(VI)/SiO_2 and W(VI)/SiO_2. The FTIR results and steady-state flow reactor data for reaction of 1-butene are discussed in terms of these pathways to isomerization.

The adsorption of 1-butene on Mo(VI)/SiO_2 and W(VI)/SiO_2 leads to the presence of two surface species. The first species is characterized by strong $\nu_{as}CH_3$, $\nu_{as}CH_2$, ν_sCH_3, and ν_sCH_2 modes at 2980, 2942, 2934, and 2865 cm^{-1}, respectively, which are characteristic of sp^3-hybridized carbon atoms (36). The adsorption of 2-butanol on Mo(VI)/SiO_2 results in a spectrum that is identical to that observed on the adsorption of 1-butene (Fig. 4); therefore, it is reasonable to assign the surface species observed on the adsorption of 1-butene on Mo(VI)/SiO_2 and W(VI)/SiO_2 to a *sec*.-butoxide species formed by the protonation of 1-butene. Brønsted acid sites on Mo(VI)/SiO_2 and W(VI)/SiO_2 (Fig. 7) would enable the protonation of 1-butene resulting in an alkoxide intermediate. The coupled C–C and C–O stretches of this species could not be observed due to the strong absorbance of the SiO_2 support below 1300 cm^{-1}. Busca and Lorenzelli have observed *sec*.-butoxide formation when butenes are adsorbed on $FeCrO_3$ (6).

The *sec*.-butoxide species does not have any absorbance in the C=C stretching region. In this region (Fig. 3), the band observed at 1611 cm^{-1} can be assigned to a second species on the surface, a π complex of 1-butene. Two conformers of 1-butene, the s-*cis* and *gauche* conformers, are distinguishable by IR, with gas phase C=C modes at 1643 and 1647 cm^{-1}, respectively (39), but a clear identification of which conformer was on the surface could not be made. The lowering of the C=C stretching mode from the gas-phase value by ~20 to 40 cm^{-1} is typical and has been reported previously for adsorption on ZnO (7). The C–H stretching modes of the π complex should be similar to those of the *sec*.-butoxide species in the region 2800 to 3000 cm^{-1}, but weaker, since only one sp^3- and one sp^2-hybridized carbon atom are present. Expected vinylic C–H modes above 3000 cm^{-1} could not be observed. Previous results have shown that such modes are typically very weak for adsorbed vinylic species. Both a *sec*.-butoxide species and a π complex of 1-butene are present on the surface of Mo(VI)/SiO_2 and W(VI)/SiO_2 at 300 K. The relative amount of π complex of 1-butene to alkoxide species is higher on the surface of W(VI)/SiO_2 than on Mo(VI)/SiO_2, based on the higher relative intensities of the 1611 cm^{-1} band and the C–H modes.

Alkoxide intermediates can eliminate H and desorb as any of the linear butenes or undergo oxidative dehydrogenation on the surface resulting in ethyl methyl ketone. Temperature evolution of the adsorbed *sec*.-butoxide intermediate on Mo(VI)/SiO_2 (Fig. 5) and W(VI)/SiO_2 results in nearly complete desorption of the same by 473 K. The π complex of 1-butene that is observed for 1-butene adsorption at 300 K on Mo(VI)/SiO_2 and W(VI)/SiO_2 has also completely desorbed by 473 K. It could not be determined if the π complex desorbs as 1-butene or if it also undergoes transformation into an alkoxide intermediate before desorption as one of the linear butenes. No IR bands characteristic of ethyl methyl ketone were observed. These results suggest that a Brønsted catalyzed pathway for isomerization of 1-butene exists over Mo(VI) and W(VI), and should be observed in flow reactor studies.

Steady-state reactivity data agree very well with infrared results. For Mo(VI)/SiO_2 (Fig. 2), the isomerization pathway at $T < 523$ K is consistent with the Brønsted catalyzed pathway where a *sec*.-butoxide species is the intermediate. Nearly complete desorption of the adsorbed alkoxide took place by 473 K in the infrared studies. At $T > 573$ K, the increase in isomerization activity of Mo(VI)/SiO_2 follows closely the onset of formation of 1,3-butadiene, a product that can be formed only via allylic C–H abstraction. So above 573 K, the isomerization activity can be attributed to the allylic pathway. In the intermediate temperature regime (473–573 K), we suggest there is a transition from the Brønsted catalyzed mechanism to the oxidative dehydrogenation mechanism. We argue below that allylic reaction pathway products accumulate on the surface, poisoning sites for reaction on the Cr catalyst, and that at a sufficiently high temperature they desorb, freeing sites for isomerization and oxidation. A similar poisoning process could account for the fall in isomerization activity of the Mo catalyst in the intermediate temperature regime.

For W(VI)/SiO_2, the demarcation of these two pathways is not as clear. The high isomerization activity observed at $T < 523$ K is consistent with a Brønsted catalyzed pathway; alkoxide intermediates are observed in IR studies at $T < 523$ K. The transition to an allylic pathway for W(VI)/SiO_2 will occur at a higher temperature than in the case of Mo(VI)/SiO_2, consistent with the onset of 1,3-butadiene formation at 623 K. Therefore, the Brønsted catalyzed pathway is still available for 1-butene isomerization at higher temperatures on W(VI)/SiO_2 than on Mo(VI)/SiO_2.

When 1-butene is adsorbed on Cr(VI)/SiO_2, three strong modes are observed initially in the νC=C region at 1611, 1637, and 1675 cm^{-1}. Subsequent temperature evolution results in complex spectra in the region 1300 to 1700 cm^{-1}, making assignments difficult. The modes of π complexes of 1-butene, *cis*-2-butene, and *trans*-2-butene are consistent with the three modes seen initially. π complexes for the butenes have been observed previously on ZnO and similar assignments were made (11). With increasing temperature, the bands at 1675 and 1611 cm^{-1} grow in intensity, with the emergence of new bands at 1590 and 1560 cm^{-1}. The increased-intensity bands at 1675 and 1611 can be assigned to the C=O and C=C stretches of the s-*trans* conformer of methyl vinyl ketone. Absence of data below 1300 cm^{-1} prevents us from making the assignments with certainty. Adsorption and temperature evolution of 1,3-butadiene on $FeCrO_3$ result in the emergence of similar bands in the region 1300 to 1700 cm^{-1} (6). In any case, methyl vinyl ketone or 1,3-butadiene can be formed only through the allylic

pathway. The very weak bands observed for sp^3-hybridized carbon atoms in the νC–H region for Cr(VI)/SiO_2, when compared with Mo(VI)/SiO_2 or W(VI)/SiO_2, suggest that unsaturated hydrocarbons are present. Thus, infrared results indicate that the allylic pathway dominates even at 300 K for Cr(VI)/SiO_2.

In steady-state reactor studies with Cr(VI)/SiO_2, isomerization is observed only with the onset of 1,3-butadiene formation at 473 K, which takes place through the allylic pathway. A Brønsted catalyzed pathway is not seen in reactor studies. While surface species, ethyl vinyl ketone or 1,3-butadiene, that are consistent with the allylic pathway are observed at 300 K in IR studies, the onset of formation of 1,3-butadiene is not seen in reactor studies until 423 K. One possible explanation for why oxidative dehydrogenation products are not observed at lower temperatures in reactor studies could be that the formation of ethyl vinyl ketone or 1,3-butadiene at the lower temperatures poisons the surface sites until desorption of these products can take place. Adsorbed ethyl vinyl ketone could also provide a pathway for nonselective oxidation of 1-butene to CO and CO_2, as has been suggested elsewhere (6).

The *cis*/*trans* ratio between 1.1 and 1.5 for the W(VI)/SiO_2 and Mo(VI)/SiO_2 catalysts at lower temperatures is consistent with a Brønsted catalyzed pathway, and similar results have been reported before for other oxide systems (4). At the higher temperatures, where we suggest that 1-butene isomerization takes place via an allylic route, *cis*/*trans* ratios of 2 or more are expected, but are not observed. The *cis*/*trans* ratios observed with Cr(VI)/SiO_2 also range between 1.2 and 1.5; only an allylic pathway to isomerization is present over Cr(VI)/SiO_2. One reason a larger amount of *cis*-2-butene was not seen at $T > 573$ K could be the subsequent reaction of the allylic intermediate, in a favorable configuration, to form 1,3-butadiene.

The Brønsted catalyzed pathway and the allylic pathway for isomerization of 1-butene are competing pathways. While all three catalysts [Cr(VI)/SiO_2, Mo(VI)/SiO_2, W(VI)/SiO_2] have some Brønsted acid sites, isomerization through a Brønsted catalyzed pathway is observed only on Mo(VI)/SiO_2 and W(VI)/SiO_2. In fact, isomerization through the Brønsted catalyzed pathway (W > Mo > Cr ~ 0) has an inverse trend with cation reducibility (Cr > Mo > W). The oxidative dehydrogenation pathway is favored by the more reducible cation, Cr. Both the acidity of the catalyst surface and the cation reducibility are important factors in determining activity and selectivity in the reaction of 1-butene.

CONCLUSIONS

Two distinct routes for isomerization of 1-butene over Mo(VI)/SiO_2 were identified: a Brønsted acid catalyzed pathway at $T < 523$ K and an oxidative dehydrogenation pathway at $T > 573$ K. For W(VI)/SiO_2, both pathways were observed but the demarcation was not as clear. For Cr(VI)/SiO_2, only an allylic pathway was observed, even at 300 K. The greater reducibility of the Cr cation compared with Mo and W cations is a possible reason for the allylic pathway being observed, even at 300 K. Temperature evolution studies indicate that the surface of Cr(VI)/SiO_2 is poisoned at lower temperatures by formation of oxidative dehydrogenation products such as methyl vinyl ketone and 1,3-butadiene.

ACKNOWLEDGMENTS

This work was supported by the U.S. Department of Energy, Office of Basic Energy Sciences, under Grant DE-FG03-95ER14570. Raman spectroscopy was performed in collaboration with I. E. Wachs and J. M. Jehng at Lehigh University.

REFERENCES

1. Dadyburjor, D. B., Jewur, S. S., and Ruckenstein, E., *Catal. Rev. Sci. Eng.* **19**, 293 (1979).
2. Kung, H. H., *Ind. Eng. Chem. Prod. Res. Dev.* **25**, 171 (1986).
3. Haber, J., *in* "New Developments in Selective Oxidation by Heterogeneous Catalysis" (B. Delmon, Ed.), Vol. 72, p. 279. Elsevier, New York, 1992.
4. Kung, H. H., "Transition Metal Oxides: Surface Chemistry and Catalysis." Elsevier, New York, 1989.
5. Ramani, N. C., Sullivan, D. L., and Ekerdt, J. G., submitted for publication.
6. Busca, G., and Lorenzelli, V., *J. Chem. Soc. Faraday Trans.* **88**, 2783 (1992).
7. Chang, C. C., Conner, W. C., and Kokes, R. J., *J. Phys. Chem.* **77**, 1957 (1973).
8. Davydov, A. A., "Infrared Spectroscopy of Adsorbed species on the Surface of Transition Metal Oxides." Wiley, New York, 1984.
9. Suarez, W., Dumesic, J., and Hill, C. G., Jr., *J. Catal.* **94**, 408 (1985).
10. Engelhardt, J., Goldwasser, J., and Hall, W. K., *J. Catal.* **70**, 364 (1981).
11. Dent, A. L., and Kokes, R. J., *J. Phys. Chem.* **75**, 487 (1971).
12. Busca, G., Ramis, G., Lorenzelli, V., Janin, A., and Lavalley, J. C., *Spectrochim. Acta A* **43**, 489 (1987).
13. Busca, G., Centi, G., Marchetti, L., and Trifiro, F., *Langmuir* **2**, 568 (1986).
14. Busca, G., Finocchio, E., Lorenzelli, V., Trombetta, M., and Rossini, S. A., *J. Chem. Soc. Faraday Trans.* **92**, 4687 (1996).
15. Escribano, V. S., Busca, G., and Lorenzelli, V., *J. Phys. Chem.* **95**, 5541 (1991).
16. Roark, R. D., Kohler, S. D., Ekerdt, J. G., Kim, D. S., and Wachs, I. E., *Catal. Lett.* **16**, 231 (1992).
17. Roark, R. D., Kohler, S. D., and Ekerdt, J. G., *Catal. Lett.* **16**, 77 (1992).
18. Roark, R. D., Narayanan, C. R., Sullivan, D. L., and Ekerdt, J. G., *Chem. Mater.* **6**, 739 (1994).
19. Bond, G. C., Flamerz, S., and Shukri, R., *Faraday Discuss. Chem. Soc.* **87**, 65 (1989).
20. Deo, G., and Wachs, I. E., *J. Phys. Chem.* **95**, 5889 (1991).
21. Hardcastle, F. D., and Wachs, I. E., *J. Mol. Catal.* **46**, 173 (1988).
22. Hu, H., Wachs, I. E., and Bare, S. R., *J. Phys. Chem.* **99**, 10897 (1995).
23. Kim, D. S., Tatibouet, J., and Wachs, I. E., *J. Catal.* **136**, 209 (1992).
24. Kim, D. S., Segawa, K., Soeya, T., and Wachs, I. E., *J. Catal.* **136**, 539 (1992).
25. Kim, D. S., Ostromecki, M., Wachs, I. E., Kohler, S. D., and Ekerdt, J. G., *Catal. Lett.* **33**, 209 (1995).

26. Kim, D. S., Wachs, I. E., and Segawa, K., *J. Catal.* **146**, 268 (1994).
27. Weckhuysen, B. M., and Wachs, I. E., *J. Phys. Chem.* **100**, 14437 (1996).
28. Rajagopal, S., Marzari, J. A., and Miranda, R., *J. Catal.* **151**, 192 (1995).
29. Kataoka, T., and Dumesic, J. A., *J. Catal.* **112**, 66 (1988).
30. Kung, M. C., and Kung, H. H., *Catal. Rev. Sci. Eng.* **27**, 425 (1985).
31. Ramis, G., Busca, G., and Lorenzelli, V., *Appl. Catal.* **32**, 305 (1987).
32. Busca, G., Saussey, H., Saur, O., Lavalley, J. C., and Lorenzelli, V., *Appl. Catal.* **14**, 245 (1985).
33. Martin, C., Martin, I., del Moral, C., and Rives, V., *J. Catal.* **146**, 415 (1994).
34. Datka, J., Turek, A.M., Jehng, J. M., and Wachs, I. E., *J. Catal.* **135**, 186 (1992).
35. Kohler, S. D., and Ekerdt, J. G., *J. Phys. Chem.* **98**, 1276 (1994).
36. Bellamy, L. J., "The Infrared Spectra of Complex Molecules," 3rd ed. Vol. 1. Chapman & Hall, New York, 1975.
37. Kline, C. H., and Turkevich, J., *J. Chem. Phys.* **12**, 300 (1944).
38. Busca, G., and Lorenzelli, V., *Mater. Chem.* **7**, 89 (1982).
39. During, J. R., and Compton, D. A. C., *J. Phys. Chem.* **84**, 773 (1980).